Automation of the image analysis for thermographic inspection

Yuri A. Plotnikov and William P. Winfree

NASA Langley Research Center, M.S. 231, Hampton, VA 23681-0001

ABSTRACT

Several data processing procedures for the pulse thermal inspection require preliminary determination of an unflawed region. Typically, an initial analysis of the thermal images is performed by an operator to determine the locations of unflawed and the defective areas. In the present work an algorithm is developed for automatically determining a reference point corresponding to an unflawed region. Results are obtained for defects which are arbitrarily located in the inspection region. A comparison is presented of the distributions of derived values with right and wrong localization of the reference point. Different algorithms of automatic determination of the reference point are compared.

Keywords: infrared thermography, image analysis, thermal contrast, inverse problem, thermal tomography

1. INTRODUCTION

Thermographic inspections of metallic and composite structures have been shown to be an effective method for detecting flaws in structures. This is a particularly promising technique for large area inspections where its noncontacting nature is particularly advantageous. It is easily applied to curved surfaces and is often the most rapid method for inspection of aircraft structural components.

A difficulty with thermographic inspections is the interpretation of the data. Setting of a simple threshold in a thermogram seldom identifies flaws due to the variability of the inspection process. To improve the probability of detecting flaws in the material, several computational techniques have been developed. Often these techniques rely on the difference between the thermal response of a flawless or sound region of a specimen and the region being inspected. The time dependence and amplitude of the difference is used to establish the existence of flaws and to determine their characteristics. This process significantly improves the probability of detecting a flaw.

The reference thermal response for a sound region can be obtained by an independent measurement on a sample known to have no flaws. A comparison of this response with the response of the inspected sample requires that experimental conditions be exactly matched. Therefore a much more common practice is to select a region of the specimen, which by some prior experience, is considered to be sound and to use this region to determine the reference response. This can be time consuming and produces some arbitrariness in the inspection since an operator is required to select the unflawed region.

This paper discusses an automated technique for the detection of the sound area of a specimen based on its thermal response. This has an advantage of reducing the arbitrariness of the inspection. In addition, automated selection of the sound region of the sample enables easy interpretation of the data.

2. THERMAL CONTRAST

One of major derived parameters of thermal data analysis is thermal contrast *C*. It enables a quantification of the difference between thermal decays above defective and sound areas. The thermal contrast could be expressed in form of subtraction or division values of thermal response above defective area T_{def} and sound area T_{soa}:

$$C = T_{def} - T_{soa}, \qquad C = \frac{T_{def}}{T_{soa}}. \tag{1}$$

Derived equations for thermal contrast use additional parameters for normalization to decrease disturbances from emissivity (equation (6.28)[1], equation (1)[2]):

$$C = \frac{T_{def}(t) - T_{def}(0)}{T_{soa}(t) - T_{soa}(0)}, \qquad C = 2\frac{\left|T_{def}(t) - T_{soa}(t)\right|}{\sigma_{def}(t) + \sigma_{soa}(t)}, \tag{2}$$

where σ_{def} and σ_{soa} are the standard deviations for the two areas.

Suppose we have a series of N thermal images taken during the observation time t_{obs} above the inspected area, and each image is a rectangular frame having $L \times M$ pixels. If there is no prior information about defects in the inspected area then it is necessary to calculate contrast as a function of thermal response for each pixel and thermal response of sound area:

$$C(i,j,k) = f\left(T(i,j,k), T_{soa}(k)\right) \tag{3}$$

for $i = 1,2,...,L$, $j = 1,2,...,M$, and $k = 1,2,...,N$. The reference response $T_{soa}(k)$ could be a value of one pixel with coordinates of (i_{ref}, j_{ref}) or an average value of several pixels in the sound area. Analysis of the contrast defined by (3) in time domain yields quantified information of the defect depth and location.

The primary separation defective and non-defective regions is usually made by an experienced operator searching for warm spots on thermal image above possible defects[3]. It is important to synthesize an automatic procedure which can initially separate the defective and reference areas for the contrast calculation and further advanced image analysis. This step will ease the process of interpretation of thermal images and automatic defect detection. In order to locate the sound area, it is desirable to find a simple algorithm which will satisfy the next requirements:

- inspected area has unknown number of defects with unknown size;
- defects can cross the borders of observed area.

Additionally, it is expected that thermographic evaluation system adjusted to match the thermal properties of the inspected subject. This includes an optimization of the sampling interval and observation time for particular material and thickness. This requirement is common for most methods applied for nondestructive evaluations.

3. ALGORITHM DESCRIPTION

A typical temperature decay on the surface after pulse heating is shown in Fig. 1a. Temperature of the sound area T_{soa} has a lower magnitude than temperature of the surface above the defect T_{def} for each moment of time t. If the thermal decay is presented by a series of frames, the needed reference point in each frame can be chosen as the pixel having the lowest value in this frame. In order to cover all time of observation, all N frames have to be taken in consideration. It can be done by summing values of the pixels with the same index i, j and finding the minimum value of the resulting sum $T_S(i,j)$. The algorithm for the reference pixel localization could be expressed as:

$$T(i_{ref}, j_{ref}) = \min\left(T_S(i,j) = \sum_{k=1}^{N} T(i,j,k) \right). \tag{4}$$

This algorithm is accurate and stable for a series of frames received during numerical simulation of thermal inspection and provides the reference point for further advanced data processing. However, its application to the real thermal data received on the thermographic acquisition system does not always produce the desired result. Fig. 1b presents the three dimensional plot which has been received after summing of 250 frames using right part of equation (4). The object of research is a plate of thickness 2.5 cm from opaque plastic with 9 square flat bottom voids milled from the back side[2]. The voids are in order 1.6 mm, 3.2 mm, 4.8 mm, 6.4 mm, 9.5 mm, 12.7 mm, 15.9 mm, 19.0 mm, and 22.2 mm below the surface. The sampling rate is approximately 1 frame per second. As can be seen from this 3D graph, the image background is severely non-uniform. It

reflects the features of infrared acquisition system with an infrared camera Inframetrics-760 and heating inhomogeneous. It is difficult to identify the defects from this image without the trend removal and smoothing procedures. Minimum value of the obtained sum is located in the nearest left corner of the observation area (Fig. 1b).

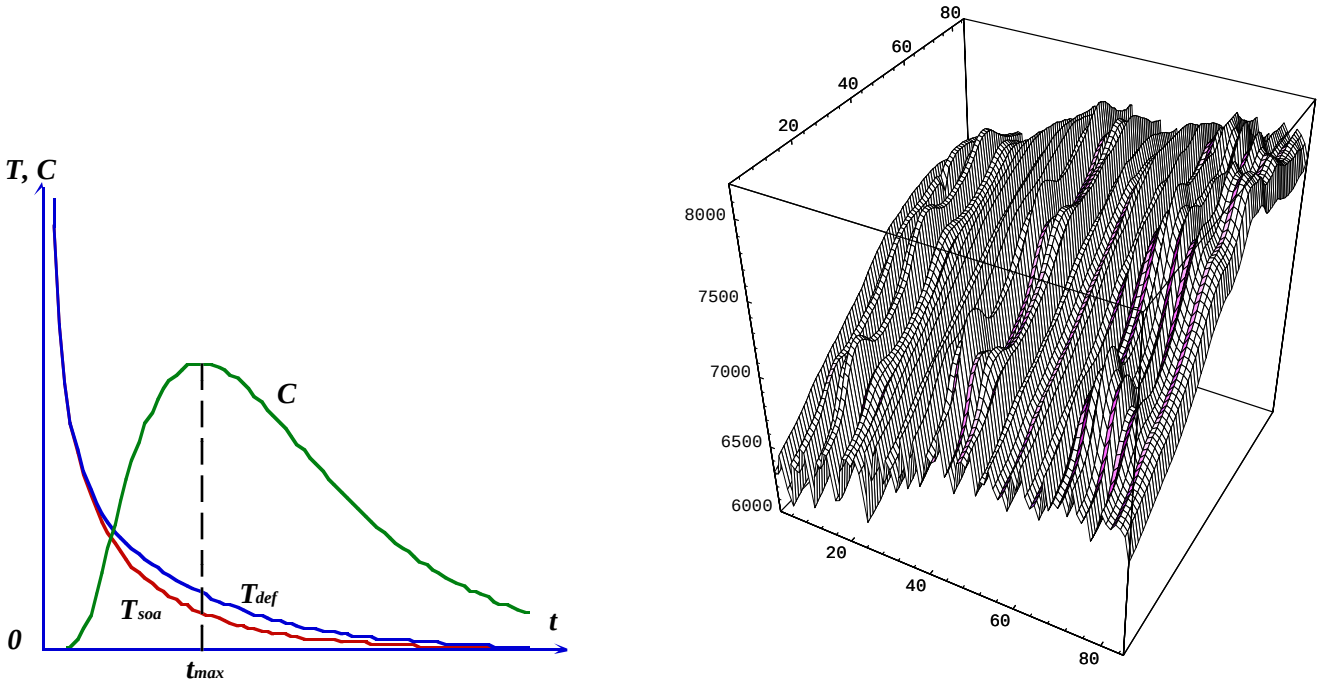

a) b)

Fig. 1. a) temperature decay $T(t)$ and contrast $C(t)$; b) three dimensional plot of summarized thermal response $T_S(i,j)$ above the plate with flat bottom holes.

To evaluate the appropriateness of the chosen reference point, the temporal dependence of the contrast has been studied. The contrast $C(i,j,k) = T(i,j,k) - T(i_{ref}, j_{ref}, k)$ has been calculated for all frames. The dependence of the contrast from the frame number k has been considered for each pixel with coordinates (i,j). Fig. 2a presents a map where gray scale represents the time of maximum for the contrast $t_{\max}(i,j)$. Black and white colors corresponds to 0 s and 250 s respectively. Since time of maximum contrast increases with the thickness of the material above the defect, the dark spots above the defects on the white background are expected. However, the timegram of the plate in Fig. 2a with the found reference point in the left lower corner (marked with the white circle) does not correspond to these expectations and does not produce understandable image of the defects made in the plate.

Another algorithm has been proposed for experimental data processing. Division the temperature response by the temperature immediately following the application of heat is a method for normalizing of the raw data. If the initial thermal distribution is homogeneous, this ratio will have lower value above the sound area since the temperature above the sound area has lower magnitude (Fig. 1a). For a series of thermal images the algorithm for the reference point localization could be expressed as:

$$T(i_{ref}, j_{ref}) = \min\left(\frac{T(i,j,k2)}{T(i,j,k1)}\right), \tag{5}$$

where $k2 > k1$. This expression carries the time processing along with spatial processing. It also has an advantage of reducing the inhomogeneoses of initial thermal distribution.

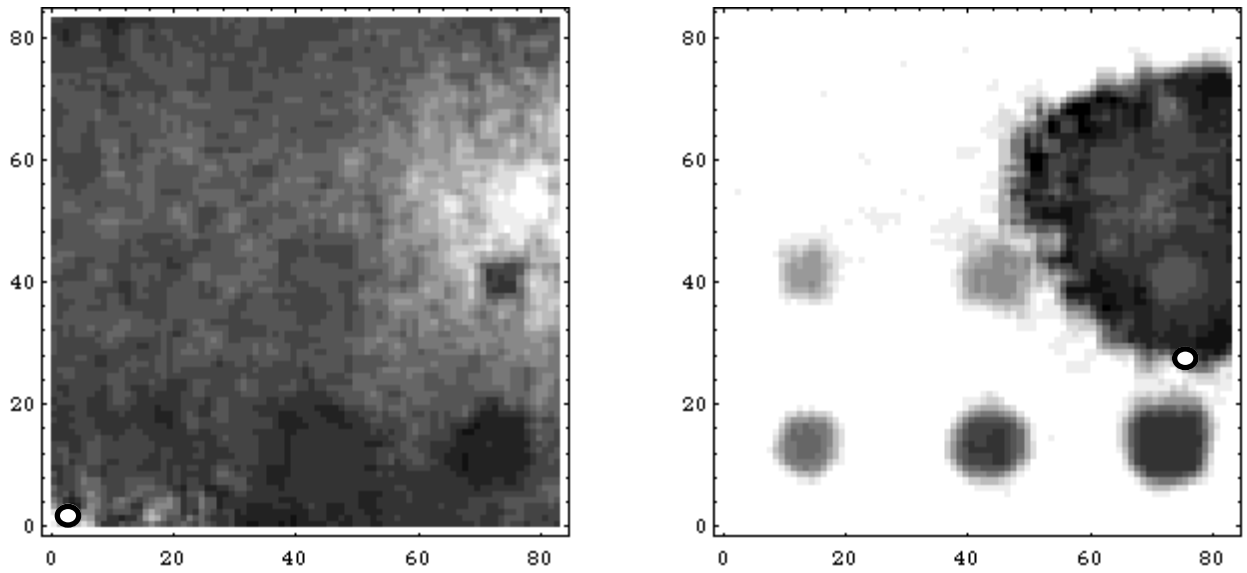

a) b)

Fig. 2. The time of the contrast maximum map, $t_{\max}(i, j)$, in gray scale (black and white colors corresponds to 0 s and 250 s respectively) for reference point location with equation (4) a) and with equation (5) b). The white circle indicates location of the reference point in the observed area.

This algorithm has been applied to the experimental data described above. A new reference pixel for thermal contrast calculation has been found with equation (5). Taking into account, that the observation time has been adjusted to the plate thickness, the next frame numbers have been selected: $k1 = 1$ and $k2 = N / 2$. The resulting timegram $t_{\max}(i, j)$ is shown in Fig. 2b. It provides the images of the 6 shallowest holes in the plate with darkness related to their depth. The large dark spot at the right central part of the timegram is not a defect and it is generated by a reflection of the flash lamp used for heating.

The method works as well with a part of observation area and when defects cross the border of the observation area. The last feature is very important for large surface to be inspected when a link between several sequential observed areas has to be done.

4. THERMAL TOMOGRAPHY

The value of each pixel of the timegram presented in Fig. 2b can be converted into the depth[3]. This calibrated image will present a distribution of all defects according to their depth. However, this image is very noisy and does not provide accurate defect sizing. The better result gives two steps thermal tomography algorithm which includes a defect edge extraction procedure following its application to the timegram[1].

In order to receive image of all defects, located in the observed area, a special program having the trend removal procedure and the defect contour detection procedure, has been applied to the summed thermal response shown in Fig. 1b. The trend removal technique uses row/column fitting algorithm[4]. The resulting smoothed thermal contrast image (Fig. 3a) is a subject of defect contour detection procedure based on the gradient contrast distribution, which has been explained in details elsewher[5]. The result of processing is a binary mask image which assigns “1” to the region detected as belonged to a defect and “0” to the defect free areas. The received mask is shown in Fig. 3b. It demonstrates all 9 flat bottom holes in the plate and their mutual location, but does not reflect square shape very well. The program does not require preliminary information about number, size, strength, and location of the defects in observed area and can be applied to a part of the image as well. A disadvantage of the applied trend removal procedure is that perimeter of analyzed region has to be defect free. This requires a human participation in the process of initial determination of the borders of the analyzed area. A trend elimination procedure using curve fitting and smoothing techniques was designed for Inframetrics-760 camera and may not work as well for other cameras.

The thermal tomogram has been received with pixel-by-pixel multiplication of the mask image and the function

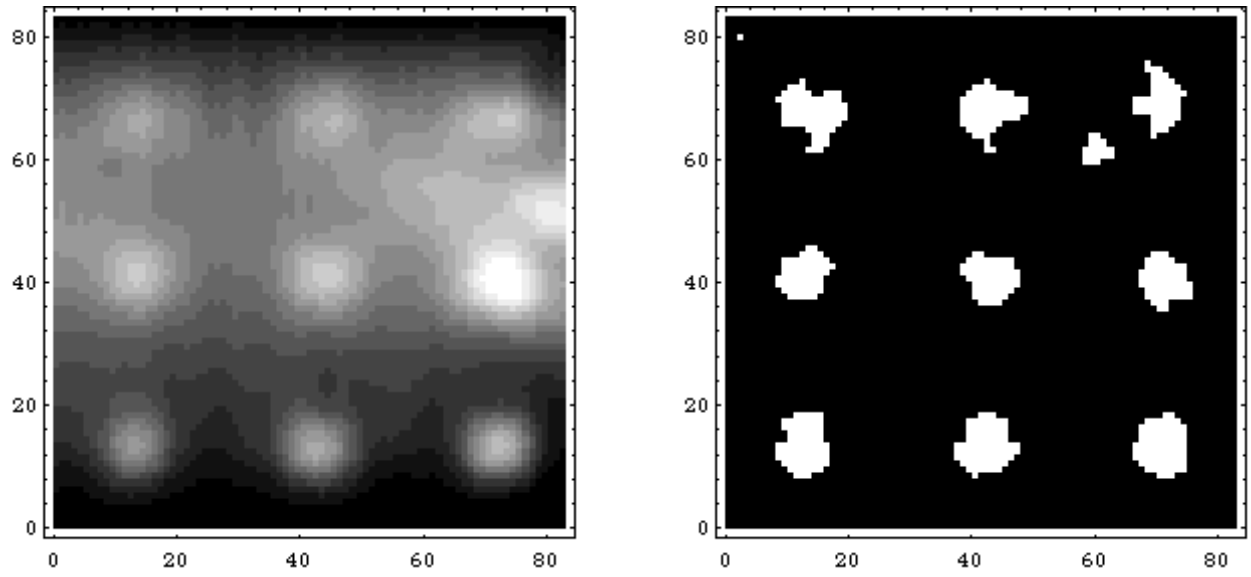

a) b)

Fig. 3. Thermal contrast image after trend removal a) and mask of the defects in the plate b).

$t_{obs} - t_{\max}(i, j)$ (in our case the observation time $t_{obs} = 250s$). The resulting 3D tomogram of the plate is shown in Fig. 4a. The false image of a defect in the upper right corner, which comes from the mask, is noticeable on the image. For comparison, the 3D outline of the plate with the artificial defects is presented in Fig. 4b.

4. CONCLUSION

An algorithm is presented for automated selection of a sound region of a specimen from its thermographic response relative to the rest of the specimen. The algorithm selects the sound regions without requiring information as to the number of defects, nor as to their size or location. The thermal response of this sound region is shown to be an effective reference for reduction of the raw thermographic data for the purpose of forming an image of the time of maximum contrast. A thermal tomography image of an inspected area can then be constructed by combining such an image with a defect contour extraction procedure. Some degree of user participation may be necessary in this latter step to insure that the perimeter of the inspected area does not coincide with any defects.

ACKNOWLEDGMENTS

This work was performed while author Plotnikov held a National Research Council - NASA Langley Research Center Research Associateship.

REFERENCES

1. X. Maldague, *Nondestructive Evaluation of Materials by Infrared Thermography*, London: Springer-Verlag, 1993.
2. W.P. Winfree and K.E. Cramer, in *Thermosense XVIII: An International Conference on Thermal Sensing and Imaging Diagnostic Applications*, Proc. SPIE Vol. 2766 (1996), pp. 228-235.
3. V. Vavilov, X. Maldague, J. Picard, R.L. Thomas, L.D. Favro, Dynamic Thermal tomography: New NDE Technique to Reconstruct Inner Solid Structure Using Multiple IR Image Processing, in: *D.O. Thompson and D.E. Chimenti (Eds), Review of progress in QNDE*, Vol. 11A, Plenum Press, N.Y., 1992, pp. 425-432.
4. E.R. Doering and J.P. Basart, Trend Removal in X-ray Images, in: *D.O. Thompson and D.E. Chimenti (Eds), Review of progress in QNDE*, Vol. 7A, Plenum Press, N.Y., 1988, pp. 785-794.
5. Y.A. Plotnikov, W. P. Winfree, Thermographic Imaging of Defects in Anisotropic Composites, in: *D.O. Thompson and D.E. Chimenti (Eds), Review of progress in QNDE*, Vol. 17, Plenum Press, N.Y., (1998, in press).

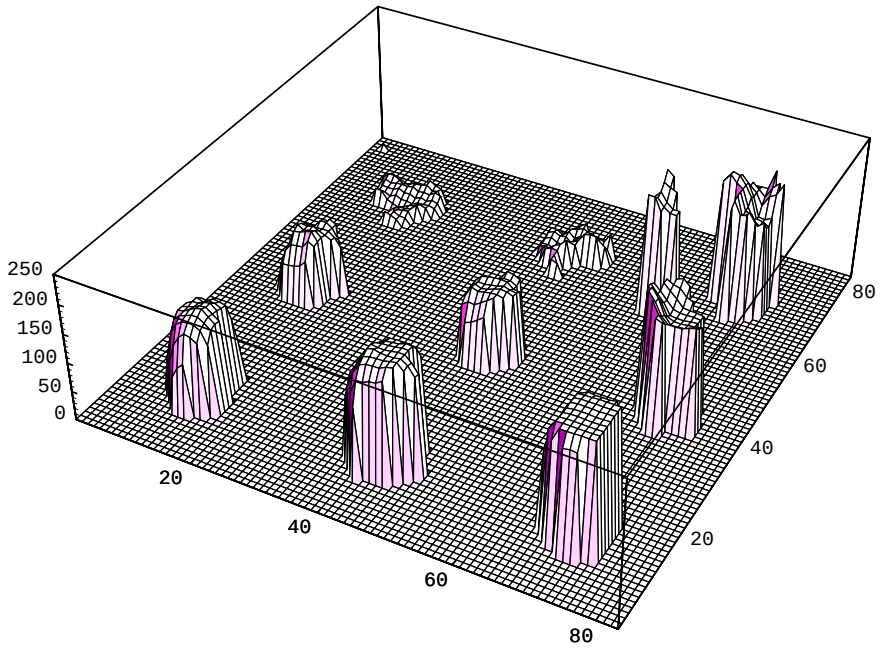

a)

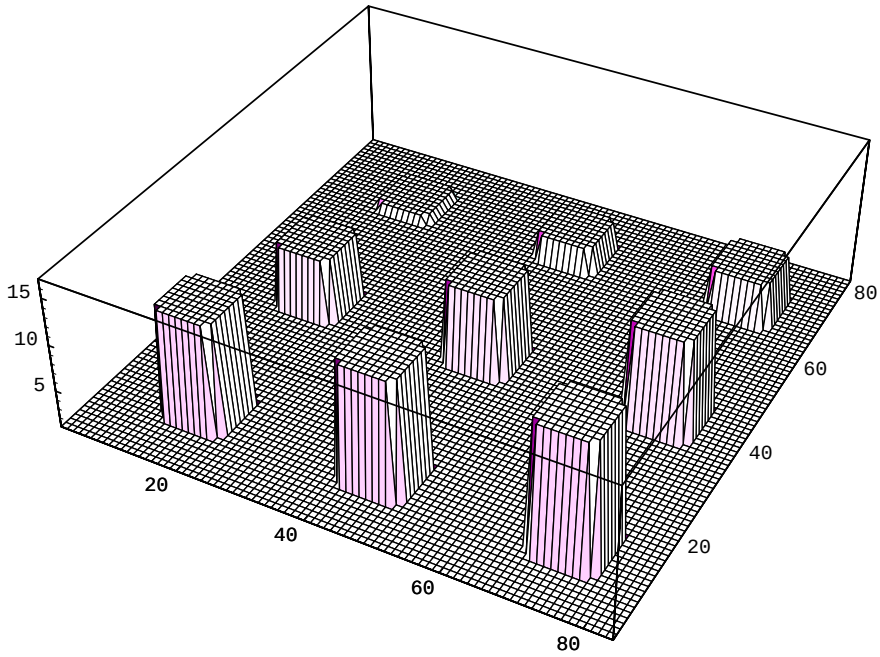

b)

Fig. 4. Tomogram of the plate using for the reference point described automatic algorithm a) and 3D outline of the plate with artificial defects (scales are different in horizontal and vertical directions) b).